Measuring Interactions between Polydimethylsiloxane and Serum Proteins at the Air–Water Interface

ARTICLE *in* LANGMUIR · JULY 2013

Impact Factor: 4.46 · DOI: 10.1021/la401619s · Source: PubMed

4 AUTHORS:

Zhengzheng Liao
University of Pennsylvania
7 PUBLICATIONS **58** CITATIONS
SEE PROFILE

Wan-Ting Hsieh
University of Pennsylvania
12 PUBLICATIONS **143** CITATIONS
SEE PROFILE

Tobias Baumgart
University of Pennsylvania
95 PUBLICATIONS **3,598** CITATIONS
SEE PROFILE

Ivan J Dmochowski
University of Pennsylvania
80 PUBLICATIONS **1,779** CITATIONS
SEE PROFILE

Langmuir

Article

pubs.acs.org/Langmuir

Measuring Interactions between Polydimethylsiloxane and Serum Proteins at the Air−Water Interface

Zhengzheng Liao,[†,§] Wan-Ting Hsieh,[†,§] Tobias Baumgart,*[,†] and Ivan J. Dmochowski*[,†]

[†]Department of Chemistry, University of Pennsylvania, 231 South 34th Street Philadelphia, Pennsylvania 19104, United States

Supporting Information

ABSTRACT: The interaction between synthetic polymers and proteins at interfaces is relevant to basic science as well as a wide range of applications in biotechnology and medicine. One particularly common and important interface is the air−water interface (AWI). Due to the special energetics and dynamics of molecules at the AWI, the interplay between synthetic polymer and protein can be very different from that in bulk solution. In this paper, we applied the Langmuir−Blodgett technique and fluorescence microscopy to investigate how the compression state of polydimethylsiloxane (PDMS) film at the AWI affects the subsequent adsorption of serum protein [e.g., human serum albumin (HSA) or immunoglobulin G (IgG)] and the interaction between PDMS and protein. Of particular note is our observation of circular PDMS domains with micrometer diameters that form at the AWI in the highly compressed state of the surface film: proteins were shown to adsorb preferentially to the surface of these circular PDMS domains, accompanied by a greater than 4-fold increase in protein found in the interfacial film. The PDMS-only film and the PDMS−IgG composite film were transferred to cover glass, and platinum−carbon replicas of the transferred films were further characterized by scanning electron microscopy and atomic force microscopy. We conclude that the structure of the PDMS film greatly affects the amount and distribution of protein at the interface.

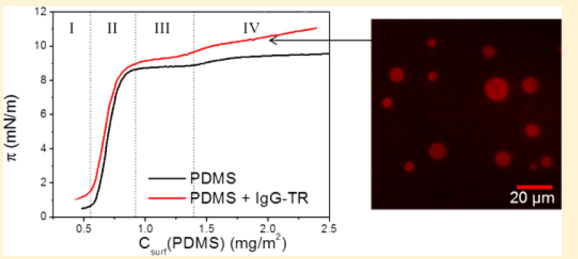

INTRODUCTION

The interaction between synthetic polymers and proteins at interfaces has broad significance in biomaterials, biosensors, and drug delivery. For example, a layer of uncharged hydrophilic polymer, such as poly(ethylene glycol), grafted to the surface of polymeric material can reduce protein adsorption efficiently, and such methods are in continuous development.[1] Conversely, protein adsorption on polymer films has been enhanced through the generation of superhydrophobic polymer surfaces or incorporation of specific protein ligands into the polymer.[2] More recently, tunable adsorption of proteins on polymer films was achieved by preferential adsorption on spatially separated chemical components that differed in hydrophobicity,[3,4] or by changing the surface charge of polymer thin films.[5,6]

The study of polymer−protein interactions at interfaces informs the ever-increasing application of synthetic polymers in biotechnical environments. Polydimethylsiloxane (PDMS) is widely used in lubricants due to its distinctive viscoelasticity, optical clarity, and low water-solubility. These properties also favor PDMS in creating microfluidic devices for demanding biotechnological and industrial applications.[7] PDMS elastomer has been widely applied in fabricating microfluidics for cell culture systems in drug discovery. Related silicone materials find increasing use in medical applications as bioengineered fluids, implant materials, and drug delivery vehicles. Silicone oil (SO), which is often composed of linear PDMS, has been employed as a temporary vitreous substitute in retinal detachment.[8] However, it was discovered recently that contact with silicone materials inhibited human corneal endothelial cell and mouse mammary fibroblast proliferation,[9,10] thus raising concerns about biocompatibility. Moreover, SO was found to induce aggregation of proteins in aqueous solution.[11] This focuses attention on SO used in pharmaceutical devices such as preloaded syringes for insulin or antibody drugs.[11−13]

Despite the prevalence of PDMS in biomedical applications, there are few studies that explore the interaction between PDMS and biopolymers from a physical−chemical perspective. The interaction between PDMS and proteins in deposited films consisting of the two components has been studied, but limited structural information could be extracted.[14,15] Besides deposited thin films on solid substrates, another approach is to use Langmuir monolayers to investigate thin-film structures at the air−water interface (AWI). Bernardini et al. applied this approach coupled with Brewster angle microscopy (BAM) to investigate the mixed film of PDMS and polymethylmethacrylate (PMMA) at the AWI and found that at a low percentage, PMMA served as a contrast enhancer and highlighted the layering transition of PDMS.[16] How these synthetic polymers interact with protein, however, has not been studied. Here, we investigated the interaction of serum proteins with PDMS at the AWI. Previously, we used a PDMS elastomer to create a chamber with a flat air−water interface for optical imaging of

Received: April 29, 2013
Revised: June 30, 2013

   dx.doi.org/10.1021/la401619s | Langmuir XXXX, XXX, XXX−XXX

fluorescently labeled proteins.[17] Lateral heterogeneity was described at the AWI that occurred in aqueous protein solution ($C_{protein}$ = 10^1–10^2 μg/mL) at neutral pH and on timescales of minutes to a few hours. More recently, we discovered that under acidic conditions (pH = 5.0) and reduced protein concentration ($C_{protein}$ = 10^{-1} to 10^0 μg/mL), unusual circular domains formed at the AWI in 1 h with dye-labeled immunoglobulin G (IgG, Figure 1A) and dye-labeled human

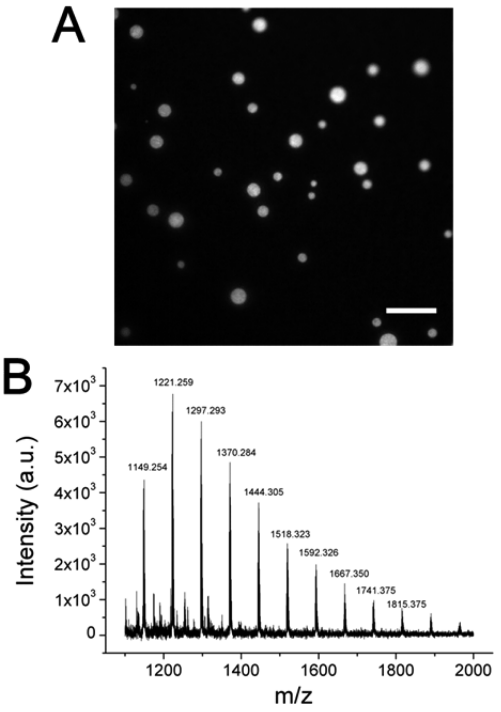

Figure 1. Circular domains formed at the air–water interface in the PDMS chamber. (A) Domains observed at the air–water interface 1 h after adding solution in the PDMS chamber. Immunoglobulin G labeled with Texas Red at 1.0 μg/mL in a 10 mM acetic acid/sodium acetate buffer (pH = 5.0). Scale bar: 20 μm. (B) MALDI-TOF mass spectrum of extracted residues from PDMS elastomer by toluene.

serum albumin (HSA, Figure S1A of the Supporting Information). At neutral pH, the circular domains formed more slowly, only appearing after overnight incubation. Such phenomena, not observed at 1 h in the solution free of contact with PDMS, but seen reproducibly in the PDMS chamber at pH = 5.0, led us to hypothesize that the circular domains were initiated by oligomers leaching from PDMS elastomer into aqueous solution, with potential for protein interaction at the AWI. MALDI-TOF mass spectrometric analysis of toluene-extracted residues from the PDMS chamber confirmed the presence of oligomers, as shown in Figure 1B. PDMS was identified with a $\Delta m/z$ of 74 between neighboring peaks, indicating the repeating $(CH_3)_2OSi$ unit. Although PDMS degradation is generally considered to be a slow process, it is known to be affected by UV irradiation, pH, and temperature.[18] Acidic conditions could catalyze hydrolysis of linear high-molecular-weight PDMS,[19] thus releasing oligomers into solution that subsequently adsorb at the AWI and compete with surface-active proteins. To investigate this phenomenon in greater detail, we explored PDMS-protein interactions at the AWI under well-controlled conditions.

Thin film structures of PDMS and IgG were formed at the AWI in order to elucidate the interaction between these two components. Using the Langmuir monolayer approach, we could control the amount of PDMS spread at the AWI and the amount of protein injected into the subphase. IgG was chosen as the model protein for the reason that it is the most abundant antibody isotype in human serum, while HSA was also used to confirm that the effect of PDMS was not specific to IgG.[20] To track the distribution of proteins in the interfacial film with optical microscopy, IgG was labeled with Texas Red (TR, see materials and methods). Combining surface pressure measurements, in situ fluorescence imaging, and topographical studies of Pt–C replica of the films transferred onto a glass surface by scanning electron microscopy (SEM) and atomic force microscopy (AFM), the structures of PDMS and mixed PDMS + protein films were investigated. On the basis of our findings, we propose a mechanistic interaction model.

RESULTS AND DISCUSSION

Surface Pressure-Surface Concentration Isotherms of PDMS and IgG-TR in Langmuir Trough. Surface pressure (π)–surface concentration (C_{surf}) isotherm measurements were performed on PDMS and PDMS + IgG mixtures. The π-C_{surf} isotherm of PDMS is shown in Figure 2A. Two marked increases in surface pressure were observed in the PDMS sample, similar to previously published results.[21−23] Two transition surface concentrations, determined from the local maximum of the first derivative of π with respect to C_{surf}, are identified as C_1 and C_2. The π-C_{surf} isotherm of PDMS was divided into four regions, and corresponding conformational models of PDMS chains have been proposed in the literature,[23,24] as summarized briefly here: Region I was defined as the region with both the lowest C_{surf} and π. Previous imaging studies showed that the polymer phase separated into quasi-two-dimensional liquid and gas phases in the millimeter-centimeter scale.[25] In region II, as C_{surf} increased, the chains compacted and formed a homogeneous liquid phase. The highly flexible Si–O chain allowed the polymer to adopt more ordered conformations with the more hydrophilic oxygen atoms immersed in the subphase and hydrophobic silicone–methyl groups sticking into the air. While most researchers agree on the chain conformation model of regions I and II, more controversy surrounds regions III and IV. Earlier studies using reflected infrared spectroscopy proposed the helix model: upon further compression from region III to IV, the helices slide onto each other, which leads to the second increase in surface pressure.[23,26] The helical structures of PDMS chains in regions III and IV are analogues of the structures found by X-ray diffraction and NMR of PDMS crystals.[27,28] On the other hand, Lee et al. found that the ellipticity of the PDMS film at the AWI changed abruptly from regions III to IV, not exhibiting a continuous transition as suggested by the helix model. Instead, the abrupt increase in ellipticity was proposed to indicate the formation of a multilayer structure.[29] This alternate model of chain conformation was further strengthened by Kim et al., who found that the vibrational sum frequency intensity in region IV was not diminished as would be expected for standing helices. Thus, they identified the Si–O chain conformation in regions III and IV as a horizontal folding model on top of the monolayer.[24] Depending on whether the chain adopts helical structure or horizontal folding, C_2 resembles the transition of chain conformation from helices to standing helices or from a single-folded layer to folded multilayer.

dx.doi.org/10.1021/la401619s | Langmuir XXXX, XXX, XXX–XXX

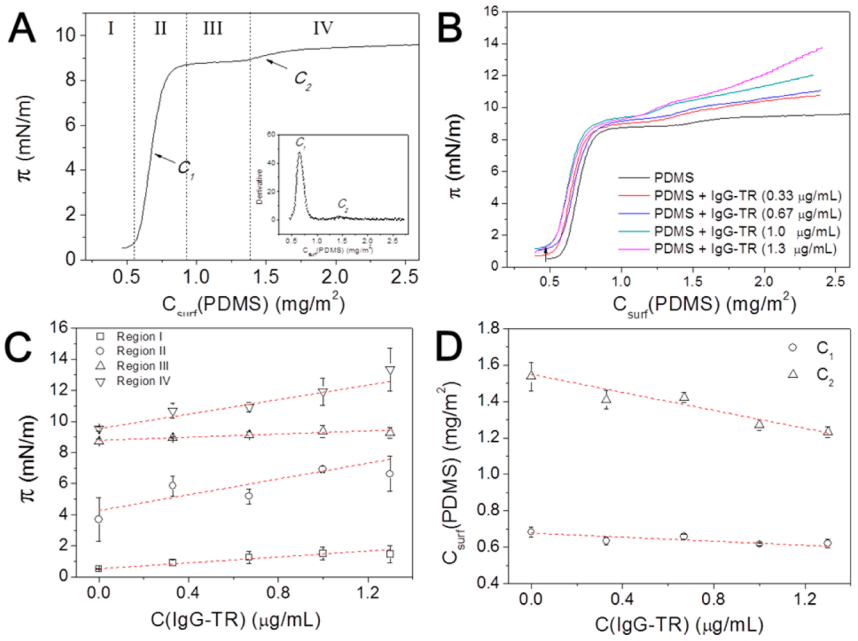

Figure 2. π-C_{surf} isotherms of PDMS and PDMS + IgG-TR. (A) π-C_{surf} isotherm of PDMS. The isotherm shown is the average of four trials. Vertical dashed lines divide the curve into four regions, I–IV, corresponding to different proposed conformations.[24] Inset shows the first derivative of the isotherm, where C_1 and C_2 correspond to the local maxima in regions II and IV. (B) Surface pressure of PDMS (spread at the air–water interface) + IgG-TR (injected into subphase) systems. Each trace of PDMS + IgG-TR is the average of three trials. (C) Surface pressure at a fixed surface concentration of PDMS in regions I–IV changed by subphase concentration of IgG-TR. Region I: 0.50 mg/m^2, region II: 0.67 mg/m^2, region III: 1.0 mg/m^2, and region IV: 2.3 mg/m^2. (D) Transition surface concentration of PDMS changed by subphase concentration of IgG-TR.

Using C_1 and C_2 as the measurement of conformational transition, we studied how the two values changed with the addition of protein. Figure 2B shows the π-C_{surf} isotherms of PDMS with Texas Red-labeled immunoglobulin G (IgG-TR) added to the subphase. PDMS was first spread at the air–buffer interface at 0.4 mg/m^2, where surface pressure remained 0 mN/m. Protein was then injected into the subphase, and the trough was left to equilibrate for 1 h. The small increase of π after 1 h indicated by the arrow in Figure 2B showed that the proteins adsorbed to the interface and resulted in a mixture of proteins and PDMS at the interfacial layer. The interfacial layer was then compressed at 10 mm/min, while surface pressure was recorded. Three parallel experiments were averaged to give each trace shown. Comparing π versus [IgG-TR] in four different regions in Figure 2C, increasing concentration of IgG-TR in the subphase led to a pronounced increase of π in regions II and IV and moderate increase in region I. In contrast, the surface pressure in region III remained constant over the range of IgG-TR concentrations studied. Furthermore, we extracted the C_{surf} of PDMS (C_1 and C_2), as well as the surface pressure at these transition points to evaluate the effect of IgG-TR on the phase transition of PDMS. Increasing subphase concentration of IgG-TR shifted C_1 and C_2 to smaller values (Figure 2D). The trend in decreasing C_1 and C_2 values indicated that IgG-TR in the interfacial layer likely reduced the available area for PDMS, and thus decreased the amount of PDMS at the interface that was necessary to undergo conformational transitions.

Circular Domains under Fluorescence Microscopy in Langmuir Monolayer. In parallel with the isotherm study, we applied fluorescence microscopy coupled to the Langmuir trough to study phase changes at the AWI. The fluorescence contrast here was from the TR dye covalently attached to the proteins. Circular domains with micrometer diameters were found in region IV during compression, as shown in Figure 3A. The same phenomenon was also observed in the PDMS + HSA-TR system (Figure S1B of the Supporting Information). The total interface fluorescence intensity (I_{inter}) shown in Figure 3B was determined from the average intensity of each pixel (I_{avg}) times the total surface area (area) of the film during the compression. Three images of randomly selected area at the AWI were analyzed to determine I_{avg}, while the total surface area was recorded by the trough system. The four regions defined by the surface pressure were indicated by dashed lines. The average intensity curve remained flat in regions I–III and then jumped significantly in region IV, a 4-fold increase. As the quantum yield of fluorophores is often solvent dependent, we measured the fluorescence intensity versus the concentration of IgG-TR dissolved in PDMS to see how the change in I_{inter} would correlate to the amount of IgG-TR in the interfacial layer, which is composed mostly of PDMS. We found that the quantum yield decreased after the concentration of dye-labeled protein reached ~5 μg/mL (Figure S2 of the Supporting Information). Because IgG-TR at the interface was in a layer of PDMS film, the solvent environment was comparable to the dye-labeled protein in PDMS. Thus, the quantity of protein at the interface in region IV exceeded that in regions I–III by at least 4-fold, considering the fluorescence quenching effect at higher concentrations. The large error bars shown in Figure 3 reflect significant sample heterogeneity at the AWI in region IV. It is worth mentioning that compression and relaxation cycles of the film area exhibited hysteresis in the surface pressure-surface concentration isotherm (data not shown here), and the segregation of proteins at the PDMS film observed at the interface was nonreversible with repetitive compression and relaxation, which could be due to the irreversible denaturation of proteins upon contact with PDMS.

dx.doi.org/10.1021/la401619s | *Langmuir* XXXX, XXX, XXX–XXX

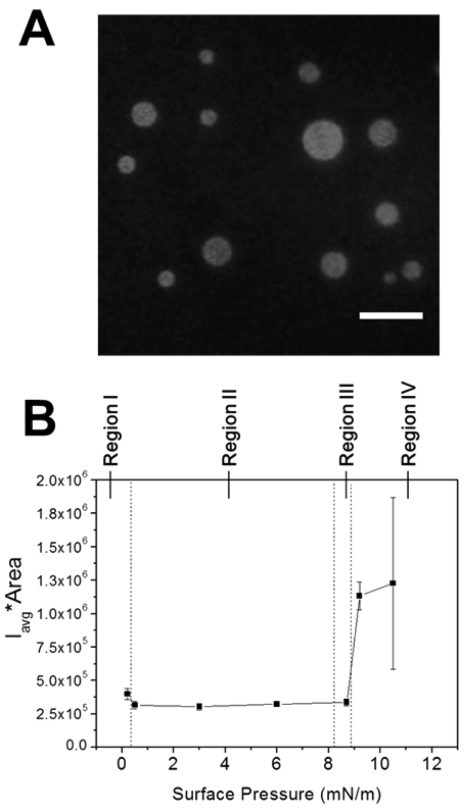

Figure 3. Fluorescence microscopy study of PDMS + IgG-TR film at the air−water interface during compression. Scale bar: 20 μm. (A) Epi-fluorescence image of the film from Texas Red channel in region IV. (B) Change of fluorescence intensity of IgG-TR at the interface with compression of the PDMS + IgG-TR (0.33 μg/mL) film.

Combining the π-C_{surf} isotherm with fluorescence imaging provided information about PDMS−protein interactions at the AWI. IgG-TR partitioned into the interfacial layer in region I, occupying available surface area between loosely packed silicone chains. The moderate increase of surface pressure in region I could be explained by minimal contact between the PDMS chain and the protein. In region II, proteins and PDMS came into closer contact with each other, thus competing for the available surface area. Because Si−O chains are highly flexible and able to reorient themselves to occupy the surface area, they likely pushed proteins into the sublayer and formed a PDMS monolayer at the interface in region III. This was demonstrated by the finding that surface pressures of PDMS + IgG-TR mixtures were close to that of the pure PDMS film in region III (Figure 2C). The protein likely remained in the sublayer close to the interface, as the total fluorescence intensity from IgG-TR remained essentially constant throughout regions I−III. The increase of surface pressure and fluorescence intensity in region IV indicated that upon further compression, a change in silicone chain conformation promoted the localization and interaction of proteins at the interface, especially at the circular domains.

Titration of IgG-TR into the Subphase. To test the hypothesis that the circular domains identified by fluorescence imaging in PDMS + IgG-TR mixtures in region IV were induced by the PDMS film as a template and then labeled by preferential adsorption of protein, we carried out a titration experiment, where PDMS stained with BODIPY was first spread at the interface at C_{surf} = 3.2 mg/m^2; π increased to 9.0 mN/m. Then IgG-TR was injected into the subphase and later adsorbed onto the PDMS film. BODIPY preferentially stains hydrophobic moieties,[30,31] and therefore traces the distribution of PDMS at the AWI through noncovalent binding. In region IV, before proteins were added to the subphase, circular domains were observed with fluorescence contrast from BODIPY in the PDMS film (Figure 4A). Similar domain

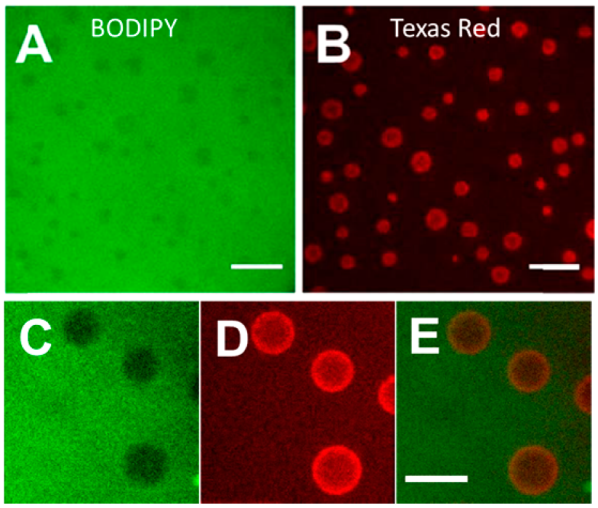

Figure 4. Fluorescence microscopy study of PDMS-only film and PDMS + IgG-TR film in region IV at the air−water interface. (A) Fluorescence image from the BODIPY channel of PDMS: C_{surf}(PDMS) = 3.2 mg/m^2, π_{trans} = 8.9 mN/m. (B) Fluorescence image from the TR channel of PDMS + IgG-TR injected into the subphase: C_{surf}(PDMS) = 3.2 mg/m^2, [IgG-TR] = 0.33 μg/mL, π_{trans} = 9.0 mN/m. (C−E) Zoomed-in micrograph of domains with BODIPY, TR, and images overlaid. Scale bar: 20 μm.

structure of PDMS (M_w = 10000 g/mol) films at the AWI was reported by Mann et al. using BAM.[32] The domains should correspond to locations with standing helices or multilayers. It is not yet clear why BODIPY preferentially partitions into the peripheral phase; one possible reason might be exclusion of the dye from densely packed polymer chains. Another dye, Sulforhodamine 101, was also used to stain PDMS and trace the distribution of polymers at the AWI. This dye was similarly excluded from the circular domains in PDMS films in region IV (Figure S3 of the Supporting Information). After injection of IgG-TR into the subphase to the concentration of 0.33−0.67 μg/mL, proteins preferentially localized to the circular domains at the interface (Figure 4B). Zoomed-in images showed heterogeneity in IgG-TR fluorescence within some of the domains. The overlay of BODIPY and IgG-TR images showed that IgG-TR tends to localize at the outer edge of PDMS circular domains (Figures 4, panels C−E). With further increase in the amount of IgG-TR injected into the subphase, the domain features disappeared and the interface became more homogeneous and dominated by TR fluorescence (Figure S4 of the Supporting Information).

We hypothesize that preferential adsorption of IgG-TR to the circular domains was due to the greater hydrophobicity of the domains in this region. It is known that proteins preferentially adsorb to more hydrophobic surfaces.[33] On films made of polymer blends, proteins such as concanavalin A have been observed to adsorb preferentially to the most hydrophobic regions.[34] For PDMS films in region IV, where the circular domains likely consist of highly compacted polymer

dx.doi.org/10.1021/la401619s | Langmuir XXXX, XXX, XXX−XXX

chains, increased hydrophobicity in the domain should favor protein adsorption.

Characterization of the Microstructure of Region IV Domains. To characterize the microstructures of domains observed in region IV, PDMS and PDMS + IgG-TR films formed at the AWI were transferred to solid substrate and replicated with a thin platinum−carbon (Pt−C) layer for SEM imaging. The PDMS or PDMS + IgG-TR films were transferred to glass coverslips through Langmuir−Schaefer approach and air-dried. The transferred samples were first imaged by fluorescence microscopy to confirm the transfer efficiency of the film for both samples (Figure 5, panels A−B). The fluorescence images showed moderate shape distortion after the transfer step, and domains were often observed at higher density close to the edges of the cover glass than in the center. Nevertheless, most features of the film were preserved on the glass substrate. Following transfer, the samples were coated with a 2.9 nm platinum film and backed with a 9.0 nm thick carbon continuous film at a 45° angle deposition with the specimen stage rotating. After replication, the Pt−C replica was gently separated from the cover glass and transferred to a clean silicon wafer surface for SEM imaging. The Pt−C replication for the electron micrograph method has been established and applied to study polymer films, protein films, and cellular components such as actin filaments in the cytoskeleton.[35,36] This method is most suitable for specimens with nonperiodic features, thus it served well in our system where the domains were scattered on the films. Figure 5, (panels C and D) show the SEM images of domains in the Pt−C replica of PDMS and PDMS + IgG-TR films, respectively.

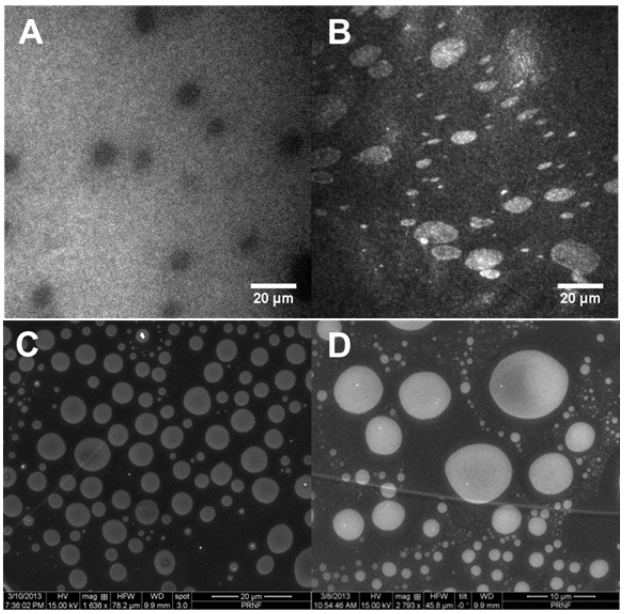

Figure 5. Characterization of transferred films on cover glass substrate. (A−B) Fluorescence microscopy images of (A) PDMS and (B) PDMS + IgG-TR film transferred on glass. (C−D) SEM images of Pt−C replica of (C) PDMS and (D) PDMS + IgG-TR transferred film.

Moreover, the Pt−C replica facilitated AFM imaging as we attempted to measure the height of the domains. Direct measurement of the domains in PDMS or PDMS + IgG-TR film on cover glass proved challenging due to the low density of domains and the high flexibility of Si−O chains. Using low magnification SEM images of the Pt−C replica as a reference map, we were able to locate the domains more reliably under the optical channel of the AFM probe. The AFM images of the replica of PDMS and PDMS + IgG-TR films are shown in Figure 6. Compared to PDMS film (Figure 6, panels A and B), PDMS + IgG-TR film (Figure 6, panels C and D) showed increased surface roughness. Figure 6E summarizes the domain height (h) measured by AFM in Pt−C replica in histograms. We define the domain height as the height difference between the domain and the peripheral areas measured by AFM. According to the chain conformation model of the PDMS film, the peripheral area should be a monolayer of PDMS, which is ∼0.7 nm in thickness.[21,29]

Here, we compared the thickness of the PDMS film (without protein) in region IV obtained with our method to that reported in the literature in order to validate the method. Using ellipsometry and neutron reflectivity, Mann et al. reported the overall film thickness of PDMS to be ∼1.4 nm at the surface concentration corresponding to region IV and showed fluctuations in the thickness of the polymer film.[21,32] Because the beam size of the reported ellipsometry experiment was ∼2 mm in diameter, the domain height obtained should represent an average value for the film. With AFM imaging of the replica of PDMS film, the average domain height was 36 ± 10 nm, which was much larger than that indicated by ellipsometry and neutron reflectivity. Nevertheless, the overall thickness of the PDMS film could be estimated, by combining the domain height measurement and area fraction of domains in the film obtained from fluorescence microscopy. By quantifying the area

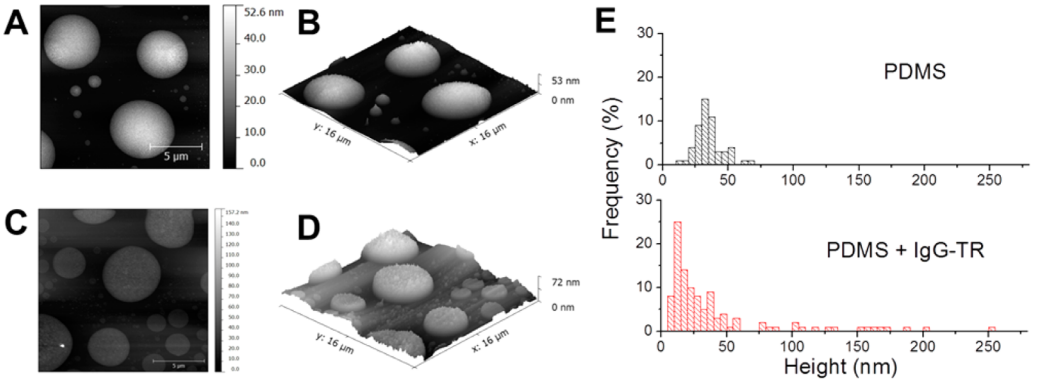

Figure 6. AFM height images and height analysis of Pt−C replicas. Representative AFM images of (A−B) PDMS and (C−D) PDMS + IgG-TR C/Pt replicas. (E) Domain height histogram of PDMS and PDMS + IgG-TR Pt−C replicas.

dx.doi.org/10.1021/la401619s | Langmuir XXXX, XXX, XXX−XXX

percentage of domains in fluorescence images of PDMS films (Figure S5 of the Supporting Information), we found the domain area accounted for 6 + 2% of the total surface area at C_{surf}(PDMS) = 3.2 mg/m^2. The overall film thickness equals domain height × domain area percentage + monolayer thickness × monolayer area percentage. This produced an overall film thickness of 2.9 + 1.0 nm, which agrees reasonably well with the thickness measured by ellipsometry and neutron reflectivity.[29] The largest source of error likely results from the area percentage of domains quantified from fluorescence imaging, as well as potential exaggeration of height differences by Pt−C coating.

In Figure 6E, the domain height of PDMS + IgG-TR showed a much larger variance than that of the PDMS film, due to partition of proteins into the film. The population of domains with h < 20 nm in PDMS + IgG-TR was significantly larger than that observed in the PDMS film, and the emergence of h > 75 nm domains was also uniquely observed. Protein partitioning into the interfacial layer was evident from comparison of the histograms (see Figure 6E). It is known that contact with silicone oil can induce protein denaturation and aggregation,[31,37,38] thus when protein adsorbed at the PDMS film, it may partially unfold or aggregate, which could contribute to the formation of the domains with h > 75 nm identified in the PDMS + IgG-TR film.

From the π-C_{surf} isotherm, fluorescence imaging, SEM, and AFM imaging of Pt−C replica of transferred films, we propose the following mechanistic model of PDMS/IgG-TR interaction at the AWI: In region I, proteins adsorbed to the free surface area between randomly oriented silicone chains, which led to the small increase in surface pressure shown in Figure 2 (panels B and C). In region II, the increase in surface pressure in the presence of protein (Figure 2C) indicated that while the silicone chains started to adopt a more ordered structure, the proteins competed for available interfacial area. In region III, the surface pressure was dominated by PDMS with minimal contributions from the protein, showing that proteins were squeezed out of the interfacial layer by ordering PDMS chains. However, the total fluorescence intensity of proteins at the interface remained comparable to region II, as shown in Figure 3B, indicating that proteins remained in the sublayer beneath the film formed by silicone chains in region III. In region IV, with further compression, the polymer conformation transitioned from a two-dimensional homogeneous layer to three-dimensional, more heterogeneous structures (Figures 4 and 6). This transition promoted protein partitioning into the film, where the protein preferentially localized to circular PDMS domains that formed.

■ CONCLUSION

In summary, we have characterized synthetic polymer−protein interactions in PDMS/IgG-TR and PDMS/HSA-TR films. This study sheds light on the complex interplay between PDMS and these proteins, and should apply broadly to other proteins and PDMS interactions in general. Our study indicates that IgG adsorption favored the condensed domain region in the PDMS film. By keeping the surface concentration of PDMS below the limit required to form domain structures in region IV (∼1.6 mg/m^2), it was possible to reduce significantly the amount of protein adsorbed at the interface, thereby reducing protein loss and denaturation at the interface. This work also provides a cautionary tale about the use of PDMS in biotechnology applications, particularly involving low concentrations of protein. Clearly, PDMS can have a profound effect on protein surface behavior and should be utilized with discretion in situations where interfacial phenomena dominate.

■ MATERIALS AND EXPERIMENTAL METHODS

Reagents. PDMS was purchased from Fisher Chemical (catalog no. S159-500). The number average molecular weight (Mn) of PDMS sample was determined by gel permeation chromatography (GPC) to be 6800 g/mol, with a polydispersity index (PDI) of 1.6, using PMMA as the standard and tetrahydrofuran as the solvent. Stock solution of PDMS was prepared by adding 5.0 μL of PDMS into 5.0 mL of chloroform (Fisher Chemical catalog no. C606-1). For fluorescence imaging, 0.2 mg/mL stock solution of BODIPY 493/503 (Life Technologies, catalog no. D-3922) was added into the PDMS solution to make a final concentration of 3.8 μM BODIPY in PDMS chloroform solution. In the case where Sulforhodamine 101 (Life Technologies, catalog no. S359) was used, the final concentration of Sulforhodamine 101 was 4.9 μM in the PDMS stock solution.

IgG and HSA (Sigma-Aldrich, catalog no. I4506 and A3782, respectively) were labeled with an amine-reactive fluorophore, Texas Red-X succinimidyl ester (Life Technologies, catalog no. T-20175). Texas Red-X succinimidyl ester was first dissolved in dimethylformamide at the concentration of 10 mg/mL, and then a certain volume of the dye solution was slowly added into the aqueous protein solution at a 10:1 dye-to-protein molar ratio while stirring. The protein solution was made by dissolving proteins (either IgG or HSA) at 2 mg/mL in 0.1 M $NaHCO_3$ buffer at pH 8.3. The vial was covered with aluminum foil and stirred continuously for 2 h at room temperature. Unreacted dye was removed by running the reaction solution through an Econo-Pac 10DG column (Bio-Rad). The labeled proteins were eluted with 10 mM phosphate buffer, pH = 7.4, and further concentrated and purified by 10 kDa cutoff molecular weight centrifugal filter units (Millipore) at 7 krpm at 4 °C for 30 min and dialyzed by 10 kDa dialysis cassettes (Thermo Scientific) against 1 L of 10 mM phosphate buffer at 4 °C for 1 week while the container was covered with aluminum foil. The final concentration of labeled protein was determined by Lowry assay[39] (Thermo Scientific) using bovine serum albumin (Thermo Scientific, cataolog no. 23209) as the standard. The number of dyes per protein was determined by the absorbance at 280 and 595 nm by UV−vis spectroscopy, using ε_{280} = 203000 cm^{-1} M^{-1} for IgG absorbance (or 36000 cm^{-1} M^{-1} for HSA absorbance) and ε_{595} = 80000 cm^{-1} M^{-1} for Texas Red absorbance, according to the protocol provided by Life Technologies. The value was typically 0.6−2.1, depending on the loss of reactivity during the storage time of the dye solution. The labeled protein solution was aliquoted and stored at −20 °C for further use.

Matrix Assisted Laser Desorption/Ionization-Time-of-Flight-Mass Spectrometry (MALDI-TOF-MS). PDMS elastomers were cut into small pieces and swelled in toluene in glass vials overnight while stirring. The solvent was evaporated under vacuum to concentrate the extract. Then 10 μL chloroform was added into the tube to redissolve the extract. Dithranol was dissolved in chloroform at 0.25 M as the matrix and silver trifluoroacetate dissolved at 1.25 M as the salt. The polymer/matrix/salt mixture was in a volume ratio 2/1/1, and 1 μL of sample was applied onto a MALDI plate and dried. MALDI-TOF-MS measurements were performed with a Bruker Daltonics Ultraflex III MALDI-TOF/TOF mass spectrometer, in a mass range of m/z 0−4000.

Langmuir−Blodgett Trough Experiment. The π-C_{surf} isotherm and titration experiment was performed with a MicroTroughXS system (Kibron Inc.). The metal trough was designed for fluorescence imaging; it has a quartz glass window in the center. Surface pressure was measured by the Du Noüy−Padday technique,[40] using the DyneProbe provided by Kibron Inc., while the surface area was controlled by a pair of Teflon barriers. Before each measurement, the trough was wiped with chloroform, and then washed with deionized water and ethanol sequentially. This procedure was repeated three times, and the surface pressure was calibrated with deionized water. The trough was then filled with buffer and π-C_{surf} isotherms of the

dx.doi.org/10.1021/la401619s | Langmuir XXXX, XXX, XXX−XXX

buffer were measured before each measurement to ensure that the increase in π was smaller than 0.2 mN/m, which indicated that surface-active contaminants had been eliminated.

Fluorescence Imaging. The fluorescence images were taken using an inverted fluorescence microscope (IX71, Olympus) with a long working distance objective (60× W/IR, NA 0.90, Olympus LUMPlanFL) equipped with an EM CCD camera (Hamamastu). A DualView imaging system (DV2, Photometrics, Tucson, AZ) was mounted in front of the CCD camera to enable simultaneous dual-color imaging. The excitation source was a continuous wavelength mercury lamp. For Texas Red or Sulforhodamine fluorescence, an excitation filter (540−580 nm) and emission filter (593−668 nm) were selected. For BODIPY, the excitation filter (450−490 nm) and emission filter (500−550 nm) were chosen.

π-C_{surf} Isotherm Measurement. Fifteen milliliters of 10 mM phosphate buffer at pH = 7.4 was used for the π-C_{surf} isotherm measurement. The surface area of buffer was first compressed to 7000 mm^2, and then 4.3 μL of 0.96 mg/mL PDMS dissolved in chloroform was spread carefully at the air−buffer interface. After waiting 20 min for chloroform to evaporate, the barriers were relaxed to the full trough area, and then compressed while the π-C_{surf} isotherm of the PDMS was recorded. For PDMS + IgG-TR systems, 250−1000 μL of 0.020 mg/mL IgG-TR aqueous solution was injected into the subphase behind the barriers at 20 min after the PDMS chloroform solution was spread at the interface. Then, the barriers were relaxed to a full trough area, and the system was allowed to sit for 1 h for the protein to adsorb to the interface. All π-C_{surf} isotherms were measured by compressing the barriers at 10 mm/min.

Titration Experiment. The same buffer as the isotherm measurement was used for the titration measurement. 0.5−10 μL of 0.96 mg/mL PDMS in chloroform solution was spread at the interface and the solvent was allowed to evaporate for 20 min, and then the surface area was compressed to 3000 mm^2. IgG-TR in phosphate solution (250 μL, 0.02 mg/mL) was injected into the subphase every hour until the final concentration of protein in the solution reached 1.3 μg/mL after 4 injections. Fluorescence images were collected every 1 h after the protein injection.

Film Transfer onto Cover Glass. Cleaned cover glass (Fisher Scientific, Catalog no. 12-545-80) was used for the film transfer. Cover glasses were sonicated for 10 min in acetone and ethanol sequentially and rinsed with ample deionized water. Then the cover glass was blown dry with compressed air. The sample film was first prepared at the AWI through the methods mentioned above, and then transferred onto the cover glass through the Langmuir−Schaefer method, by approaching the AWI from the air phase and touching the interface for 5 s then pulling up slowly. Excessive solution on the glass was removed by a piece of Kimwipe paper gently touching the side of the cover glass, and then the sample film on the cover glass was left to dry in the air covered by a Petri dish. The transferred film was imaged under the fluorescence microscope to check transfer quality before further characterization.

Pt−C Replication and SEM Imaging. The Pt−C replication was done following a standard procedure detailed in the literature.[41] A 2.9 nm thick Pt film was deposited and then backed by a 9.0 nm thick C film at a 45° angle deposition with the specimen stage rotating in a vacuum evaporator. The replica was released from the cover glass by floating the cover glass on 10% HF acid, which dissolves the glass after 2−3 h. Then the replica was washed by floating on highly diluted (10^{-6} by volume) household soap solution for 5 s, on bleach solution (also 10^{-6} by volume) for 30 min and on water, sequentially, and finally mounted on clean 1 × 1 cm prime-grade silicon wafer (Silicone Quest International Catalog no. 808-007). The purpose of the soap solution was to reduce the surface tension difference between HF and water to prevent the breakage of the replicas, and the bleach served to further dissolve organic materials including PDMS and protein.[42] Scanning electron microscope (SEM) images were taken with a Quanta 600 FEG Mark II system at a 15 kV accelerating voltage.

AFM Imaging. Pt−C replicas of PDMS and PDMS + IgG-TR films were also measured by atomic force microscope (Dimension 3100, Veeco/Bruker) in tapping mode with aluminum reflex coating cantilevers (Budget Sensors, Catalog no. Multi75AI). The AFM cantilever had a resonant frequency at 75 kHz and a force constant of 3 N/m. Height profiles were analyzed using WSxM 5.0,[43] and 3D AFM images were constructed using Gwyddion software.[44]

■ ASSOCIATED CONTENT

Supporting Information

Domains observed at the AWI with human serum albumin, fluorescence intensity of IgG-TR, fluorescence microscopy images of PDMS film, titration of IgG-TR in the subphase, and calculations of the domain area percentage from fluorescence images (Figures S1−S5, respectively). This material is available free of charge via the Internet at http://pubs.acs.org.

■ AUTHOR INFORMATION

Corresponding Author

*T.B.: e-mail, baumgart@sas.upenn.edu. I.J.D.: e-mail, ivandmo@sas.upenn.edu.

Author Contributions

§These authors contributed equally to this work.

Notes

The authors declare no competing financial interest.

■ ACKNOWLEDGMENTS

The authors gratefully acknowledge the support of NSF CAREER award CBET 1053857 (to T.B.) and NSF CAREER award CHE 0548188 (to I.J.D.). The authors thank the UPenn Nano/Bio Interface Center for access to its instruments, Matthew Brukman for support with AFM, Dr. Steven Jones for assistance in Pt−C coating, Zhaoxia Qian for help in SEM, Dr. Nga Hang Nguyen for conducting GPC measurements, and Dr. Zahra Fakhraai and Ethan Glor for helpful discussions.

■ REFERENCES

(1) Choi, C.; Hwang, I.; Cho, Y. L.; Han, S. Y.; Jo, D. H.; Jung, D.; Moon, D. W.; Kim, E. J.; Jeon, C. S.; Kim, J. H.; Chung, T. D.; Lee, T. G. Fabrication and characterization of plasma-polymerized poly-(ethylene glycol) film with superior biocompatibility. *ACS Appl. Mater. Interfaces* **2013**, *5*, 697−702.

(2) Elbert, D. L.; Hubbell, J. A. Surface treatments of polymers for biocompatibility. *Annu. Rev. Mater. Sci.* **1996**, *26*, 365−394.

(3) Lau, K. H. A.; Bang, J.; Kim, D. H.; Knoll, W. Self-assembly of protein nanoarrays on block copolymer templates. *Adv. Funct. Mater.* **2008**, *18*, 3148−3157.

(4) Kidambi, S.; Chan, C.; Lee, I. Tunable resistive m-dPEG acid patterns on polyelectrolyte, multilayers at physiological conditions: Template for directed deposition of biomacromolecules. *Langmuir* **2008**, *24*, 224−230.

(5) Eloi, J.-C.; Jones, S. E. W.; Poór, V.; Okuda, M.; Gwyther, J.; Schwarzacher, W. Electrochemically triggered selective adsorption of biotemplated nanoparticles on self-assembled organometallic diblock copolymer thin films. *Adv. Funct. Mater.* **2012**, *22*, 3273−3278.

(6) Pernites, R. B.; Santos, C. M.; Maldonado, M.; Ponnapati, R. R.; Rodrigues, D. F.; Advincula, R. C. Tunable protein and bacterial cell adsorption on colloidally templated superhydrophobic polythiophene films. *Chem. Mater.* **2012**, *24*, 870−880.

(7) McDonald, J. C.; Duffy, D. C.; Anderson, J. R.; Chiu, D. T.; Wu, H. K.; Schueller, O. J. A.; Whitesides, G. M. Fabrication of microfluidic systems in poly(dimethylsiloxane). *Electrophoresis* **2000**, *21*, 27−40.

(8) Skorpik, C.; Menapace, R.; Gnad, H. D.; Paroussis, P. Silcione oil implantation in penetrating injuries complicated by PVR-results from 1982 to 1986. *Retina-The Journal of Retinal and Vitreous Diseases* **1989**, *9*, 8−14.

(9) Yang, C. S.; Chen, K. H.; Hsu, W. M.; Li, Y. S. Cytotoxicity of silicone oil on cultivated human corneal endothelium. *Eye* **2008**, *22*, 282−288.
(10) Paguirigan, A. L.; Beebe, D. J. From the cellular perspective: exploring differences in the cellular baseline in macroscale and microfluidic cultures. *Integr. Biol.* **2009**, *1*, 182−195.
(11) Jones, L. S.; Kaufmann, A.; Middaugh, C. R. Silicone oil induced aggregation of proteins. *J. Pharm. Sci.* **2005**, *94*, 918−927.
(12) Thirumangalathu, R.; Krishnan, S.; Ricci, M. S.; Brems, D. N.; Randolph, T. W.; Carpenter, J. F. Silicone oil- and agitation-induced aggregation of a monoclonal antibody in aqueous solution. *J. Pharm. Sci.* **2009**, *98*, 3167−3181.
(13) Bee, J. S.; Randolph, T. W.; Carpenter, J. F.; Bishop, S. M.; Dimitrova, M. N. Effects of surfaces and leachables on the stability of biopharmaceuticals. *J. Pharm. Sci.* **2011**, *100*, 4158−4170.
(14) Bartzoka, V.; Brook, M. A.; McDermott, M. R. Protein-silicone interactions: How compatible are the two species? *Langmuir* **1998**, *14*, 1887−1891.
(15) Anderson, A. B.; Robertson, C. R. Absorption spectra indicate confirmational alteration of myoglobin adsorbed on polydimethylsiloxane. *Biophys. J.* **1995**, *68*, 2091−2097.
(16) Bernardini, C.; Stoyanov, S. D.; Cohen Stuart, M. A.; Arnaudov, L. N.; Leermakers, F. A. M. PMMA highlights the layering transition of PDMS in langmuir films. *Langmuir* **2011**, *27*, 2501−2508.
(17) Liao, Z. Z.; Lampe, J. W.; Ayyaswamy, P. S.; Eckmann, D. M.; Dmochowski, I. J. Protein assembly at the air-water interface studied by fluorescence microscopy. *Langmuir* **2011**, *27*, 12775−12781.
(18) Hillborg, H.; Gedde, U. W. Hydrophobicity changes in silicone rubbers. *IEEE Trans. Dielectr. Electr. Insul.* **1999**, *6*, 703−717.
(19) Kaali, P.; Momcilovic, D.; Markström, A.; Aune, R.; Czel, G.; Karlsson, S. Degradation of biomedical polydimethylsiloxanes during exposure toin vivobiofilm environment monitored by FE-SEM, ATR-FTIR, and MALDI-TOF MS. *J. Appl. Polym. Sci.* **2010**, *115*, 802−810.
(20) *Antibodies: A Laboratory Manual*; Harlow, E.; Lane, D., Eds.; Cold Spring Harbor Laboratory: Cold Spring Harbor, NY., 1988.
(21) Mann, E. K.; Langevin, D. Poly(dimethylsiloxane) molecular layers at the surface of water and of aqueous surfactant solutions. *Langmuir* **1991**, *7*, 1112−1117.
(22) Lenk, T. J.; Lee, D. H. T.; Koberstein, J. T. End group effects on monolayers of functionally-terminated poly(dimethylsiloxanes) at the air-water interface. *Langmuir* **1994**, *10*, 1857−1864.
(23) Mehta, S. C.; Somasundaran, P.; Maldarelli, C.; Kulkarni, R. Effects of functional groups on surface pressure-area isotherms of hydrophilic silicone polymers. *Langmuir* **2006**, *22*, 9566−9571.
(24) Kim, C.; Gurau, M. C.; Cremer, P. S.; Yu, H. Chain conformation of poly(dimethyl siloxane) at the air/water interface by sum frequency generation. *Langmuir* **2008**, *24*, 10155−10160.
(25) Mann, E. K.; Henon, S.; Langevin, D.; Meunier, J. Molecular layers of a polymer at the free water surface: Microscopy at the Brewster angle. *J. Phys. II* **1992**, *2*, 1683−1704.
(26) Hahn, T. D.; Hsu, S. L.; Stidham, H. D. Reflectance infrared spectroscopic analysis of polymers at the air−water interface. 4. Microstructure of poly(dimethylsiloxane). *Macromolecules* **1997**, *30*, 87−92.
(27) Damaschun, G. X-ray Investigation of the Structure of Silicone Rubber. *Kolloid-Zeitschrift & Zeitschrift für Polymere* **1962**, *180*, 65−67.
(28) Schilling, F. C.; Gomez, M. A.; Tonelli, A. E. Solid state NMR observations of the crystalline conformation of poly(dimethylsiloxane). *Macromolecules* **1991**, *24*, 6552−6553.
(29) Lee, L. T.; Mann, E. K.; Langevin, D.; Farnoux, B. Neutron reflectivity and ellipsometry studies of a polymer molecular layer spread on the water surface. *Langmuir* **1991**, *7*, 3076−3080.
(30) Karolin, J.; Johansson, L. B. A.; Strandberg, L.; Ny, T. Fluorescence and absorption spectroscopic properties of dipyrrometheneboron difluoride (BODIPY) derivatives in liquids, liquid membranes, and proteins. *J. Am. Chem. Soc.* **1994**, *116*, 7801−7806.
(31) Ludwig, D. B.; Trotter, J. T.; Gabrielson, J. P.; Carpenter, J. F.; Randolph, T. W. Flow cytometry: A promising technique for the study of silicone oil-induced particulate formation in protein formulations. *Anal. Biochem.* **2011**, *410*, 191−199.
(32) Mann, E. K.; Lee, L. T.; Henon, S.; Langevin, D.; Meunier, J. Polymer surfactant films at the air-water interface 1. Surface pressure, ellipsometry, and microscopic studies. *Macromolecules* **1993**, *26*, 7037−7045.
(33) Patel, A. J.; Varilly, P.; Jamadagni, S. N.; Acharya, H.; Garde, S.; Chandler, D. Extended surfaces modulate hydrophobic interactions of neighboring solutes. *Proc. Natl. Acad. Sci. U.S.A.* **2011**, *108*, 17678−17683.
(34) Zema, J.; Rysz, J.; Budkowski, A.; Awsiuk, K. Proteins grouped into a variety of regular micro-patterns by substrate-guided domains of self-assembling poly(ethylene oxide)/polystyrene blends. *Soft Matter* **2012**, *8*, 5550−5560.
(35) Ruben, G. C. Vertical Pt-C replication for TEM, a revolution in imaging non-periodic macromolecules, biological gels and low-density polymer networks. *Micron* **1998**, *29*, 359−396.
(36) Shutova, M.; Yang, C. S.; Vasiliev, J. M.; Svitkina, T. Functions of nonmuscle myosin II in assembly of the cellular contractile system. *PLoS One* **2012**, *7*, e40814.
(37) Walder, R.; Schwartz, D. K. Dynamics of protein aggregation at the oil−water interface characterized by single molecule TIRF microscopy. *Soft Matter* **2011**, *7*, 7616−7622.
(38) Zelisko, P. M.; Flora, K. K.; Brennan, J. D.; Brook, M. A. Water-in-silicone oil emulsion stabilizing surfactants formed from native albumin and alpha,omega-triethoxysilylpropyl-polydimethylsiloxane. *Biomacromolecules* **2008**, *9*, 2153−2161.
(39) Lowry, O. H.; Rosebrough, N. J.; Farr, A. L.; Randall, R. J. Protein measurement with the folin phenol reagent. *J. Biol. Chem.* **1951**, *193*, 265−275.
(40) Padday, J. F.; Pitt, A. R.; Pashley, R. M. Menisci at a free liquid surface-surface tension from maximum pull on a rod. *J. Chem. Soc., Faraday Trans. 1* **1975**, *71*, 1919−1931.
(41) Svitkina, T. Imaging cytoskeleton components by electron microscopy. *Methods Mol. Biol.* **2009**, *586*, 187−206.
(42) Svitkina, T.: Electron microscopic analysis of the leading edge in migrating cells. In *Cellular Electron Microscopy*; McIntosh, J. R., Ed.; Elsevier Academic Press Inc: San Diego, 2007; Vol. *79*; pp 295−319.
(43) Horcas, I.; Fernandez, R.; Gomez-Rodriguez, J. M.; Colchero, J.; Gomez-Herrero, J.; Baro, A. M. WSXM: A software for scanning probe microscopy and a tool for nanotechnology. *Rev. Sci. Instrum.* **2007**, *78*, 013705.
(44) Necas, D.; Klapetek, P. Gwyddion: an open-source software for SPM data analysis. *Cent. Eur. J. Phys.* **2012**, *10*, 181−188.